Broad-Band Cavity-Backed and Capacitively Probe-Fed Microstrip Patch Arrays

Miguel A. González de Aza, Juan Zapata, *Member, IEEE*, and José A. Encinar, *Member, IEEE*

***Abstract*—In this paper, a hybrid full wave method for the analysis of probe-fed infinite phased arrays of single and stacked microstrip patches, backed by metallic cavities, is applied to investigate the combined utilization of the capacitive probe-feeding technique and the cavity enclosure of microstrip patches. The goal is to obtain broad-band microstrip antennas on thick substrates without the limitations due to the generation of surface waves of the conventional microstrip antennas on infinite substrates. A design procedure for the capacitive coupling is investigated and theoretical results for the active input impedance and radiation characteristics of different wide-band antenna designs are presented.**

***Index Terms*—Capacitive probe feeding, microstrip antenna arrays.**

I. Introduction

MICROSTRIP antennas possess attractive properties and an increasing number of applications. However, it is well known that in many cases, one of the principal disadvantages of the conventional microstrip antenna configurations (single microstrip patches on thin substrates) is their narrow impedance bandwidth. Different methods based on parasitic elements, appropriate impedance-matching networks, or the utilization of lossy materials have been developed to overcome this drawback [1]. The simpler means of improving the frequency band characteristic is to increase the thickness of the substrate between the single patches and the ground plane. However, this procedure gives rise to another problems owing to the surface wave generation. Thus, as the substrate becomes thicker the radiation efficiency decreases and the antenna radiation pattern or polarization characteristics may deteriorate due to the spurious radiation. In the case of arrays, the increase of the mutual coupling between elements impedes a good impedance matching between the microstrip patches and the feed lines, as the array is scanned [2]. Additionally, for a coaxial-probe feeding the input impedance of the patch on electrically thick substrates becomes excessively inductive and leads to an undesirable mismatch [3].

In the last years, microstrip patch antennas backed by metallic cavities have been proposed to prevent surface wave modes [4]. This configuration allows to utilize thick substrates without the limitation in the scanning range, or even to achieve a considerable improvement in scan performance. To analyze these structures simple approaches become inaccurate and full-wave methods have been proposed, such as integral equation formulation [4], finite-element method [5], or hybrid techniques [6], [7].

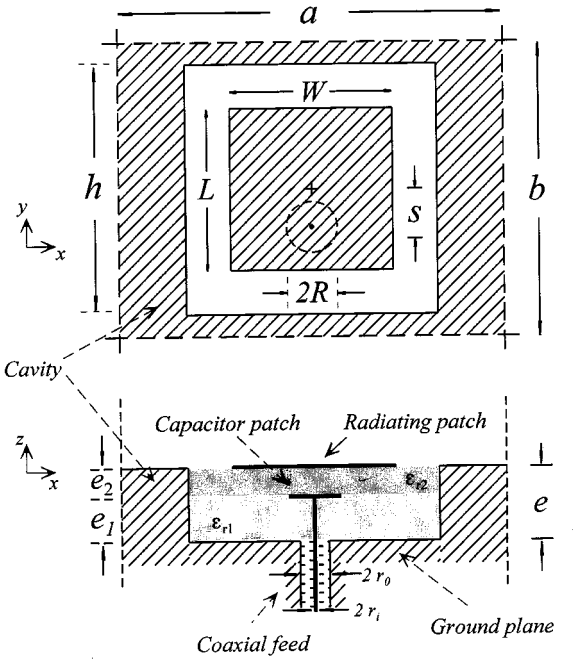

Fig. 1. Elementary cell of a capacitive probe-fed infinite array of cavity backed square patches. $a = b = 1.95$ cm, $h = 1.85$ cm, $L = W = 1.35$ cm, $s = 4.45$ mm. Coaxial feed (SMA connector): $\varepsilon_{rx} = 1.951$; $r_i = 0.64$ mm; $r_o = 2.05$ mm.

On the other hand, in the case of coaxial probe-fed microstrip antennas on electrically thick substrates, the use of the capacitive coupling within the radiating structure itself, has been investigated [8], [9] in order to compensate the probe inductance. This feeding technique is analyzed in [8] using approximate formulas or in [9] from experimental results. A simplified model for the capacitive feed based on a uniform or sine function current distribution on the probe is employed in [10]. However, simple approaches developed for thin substrates become inaccurate for electrically thick antennas and a rigorous modeling is required to take into account the effect of the probe size, the actual current variations, and the field alteration on the coaxial aperture when this is not negligible.

In this work, single microstrip patch arrays enclosed in metallic cavities and placed on thick substrates of very low permittivity materials are combined with the application of the capacitive probe feeding in place of the direct junction probe-radiating patch, as shown in the microstrip antenna

Manuscript received August 5, 1998; revised February 17, 2000. This work was supported by the Spanish "Comisión Interministerial de Ciencia y Tecnología" (CICYT) under project TIC98-0929-C02-01.

The authors are with the Departamento de Electromagnetismo y Teoría de Circuitos, ETSI de Telecomunicación, Universidad Politécnica de Madrid, Madrid, 28040 Spain.

Publisher Item Identifier S 0018-926X(00)04370-2.

TABLE I
DIFFERENT CASES CONSIDERED FOR THE CAPACITIVE COUPLING IN FIG. 1

Case	Substrate thickness with probe e_1 (mm)	Gap substrate thickness e_2 (mm)	Capacitor patch radius R (mm)	Patch displacement D (mm)
(a)	direct junction probe-radiating patch (e_1=6 mm)			0.0
(b)	4.4	1.6	2.05	0.0
(c)	5.34	0.66	1.3	0.0
(d)	5.88	0.12	0.64	0.0
(e)	case (c)			1.0
(f)	case (d)			1.5

structure of Fig. 1. The objective is to enhance the impedance bandwidth performance without an exterior matching network and without the aforementioned detrimental effects owing to the surface wave excitation.

II. METHOD OF ANALYSIS

The geometry of the capacitive probe-fed microstrip antenna considered in this paper is described in Fig. 1. It represents the unit cell of an infinite array of single square patches backed by metallic cavities. The electromagnetic coupling is performed by a circular patch with radius R (capacitor patch) connected to the inner conductor of a coaxial line. This patch is placed on a thick dielectric substrate with a thickness e_1 and separated from the radiating patch by a thin substrate layer of thickness e_2. The resultant structure may be considered as a dual layer microstrip array of patches in stacked configuration, although the capacitor patch does not operate as a radiating element on the working frequencies.

The proposed structure is analyzed by a full wave method for probe-fed and multilayered infinite phased arrays of cavity-backed and arbitrarily shaped microstrip patches in single or stacked configuration, presented recently in [11]. It is a modular procedure that combines the mode-matching (MM), generalized scattering matrix (GSM) techniques, and the two-dimensional finite-element method (2-D FEM). The analysis is limited to a single unit cell of the array from the infinite array approach and is based on the consideration of the elementary cell as an open-ended succession of homogeneous waveguides of diverse cross sections, with the same direction of propagation (z axis in Fig. 1) radiating into half-space. The radiated field is expressed as a Floquet's harmonic expansion and a modal representation, either analytical or numerical, is used in the homogeneous waveguides. Each transition between waveguides and the interface between the infinite array of apertures and the free half-space, are solved by the MM technique to obtain their individual generalized scattering matrices. A hybrid MM-FEM procedure is used for the analysis of discontinuities that involve homogeneous waveguides of arbitrary cross section. A cascade connection process for the GSM's of the waveguide discontinuities and the aperture provides the GSM of the overall structure

$$\begin{bmatrix} B^i \\ B^j \end{bmatrix} = \begin{bmatrix} S_{11} & S_{12} \\ S_{21} & S_{22} \end{bmatrix} \begin{bmatrix} A^i \\ A^j \end{bmatrix} \tag{1}$$

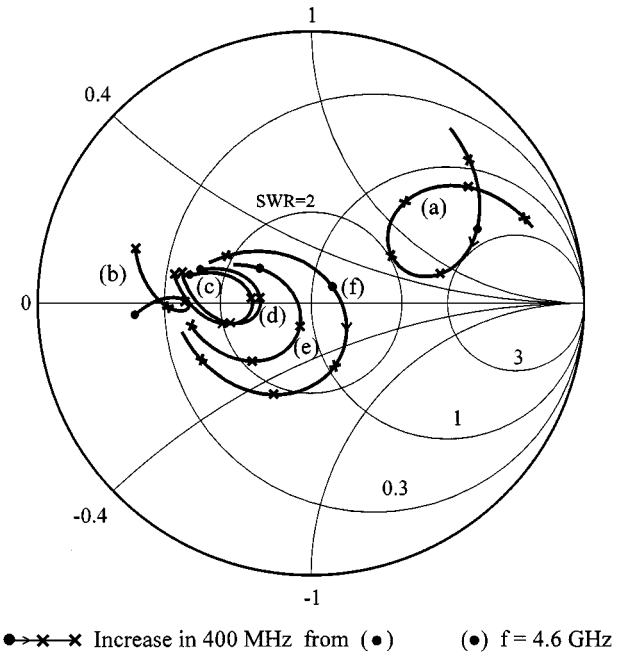

Fig. 2. Active input impedance of the infinite array defined in Fig. 1 for different cases described in Table I.

which relates incident (A) and scattered (B) modes in the coaxial line (i) and Floquet's harmonics in the half-space (j) and characterizes the array. The reflection coefficient for the TEM mode in the coaxial line $S_{11}(1, 1)$ gives the active reflection coefficient of the infinite array. In this way, the method provides a rigorous modeling of the probe feeding, allowing accurate predictions of the active input impedance, particularly in the analysis of cavity-backed arrays involving thick substrates as in the proposed structure. The active element pattern of the array is obtained from its GSM computed previously, with the method described in [12] based on an identification with the Floquet's harmonics coefficients. This technique allows to obtain in a rigorous way the field and power patterns and it is applicable even when grating lobes and losses are present. The validation of the employed analysis procedure was carried out in [11] and [12]. Input impedance and active element pattern results were presented and compared with measurements performed on waveguide simulator and other experimental data and numerical predictions previously published.

III. NUMERICAL RESULTS

A. Capacitive-Probe Feeding and Design Procedure

In a capacitive probe-fed microstrip patch antenna on a thick dielectric substrate, the probe reactance is canceled by a series capacitor placed within the same radiating structure. As is described in [8], the series capacitance value is determined by the capacitor patch size (radius R in Fig. 1) and the permittivity and thickness of the gap substrate (e_2, ε_{r2}). The reactance compensation is also associated with a reduction in the input resistance and a shift of the resonant frequency [10].

In this section, the infinite array described in the Fig. 1 has been analyzed by varying the parameters of the capacitive coupling to illustrate the adaptative effect of this feeding technique

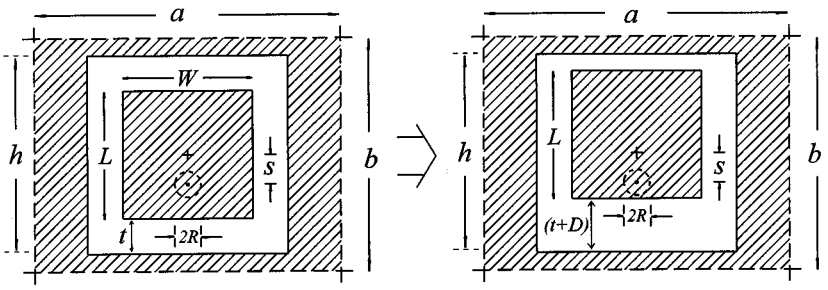

Fig. 3. Radiating patch displacement (D) toward the wall cavity for the purpose of matching the input impedance.

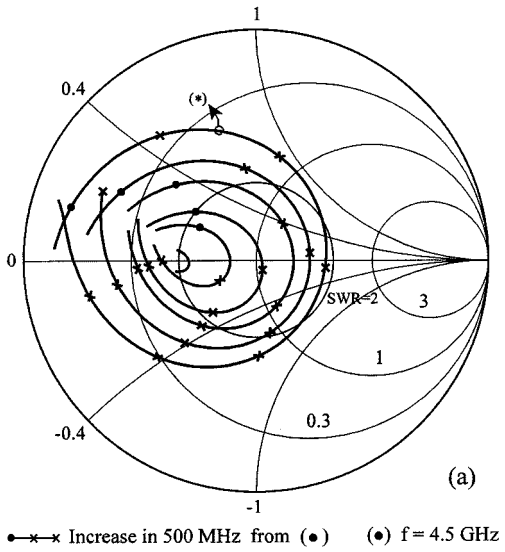

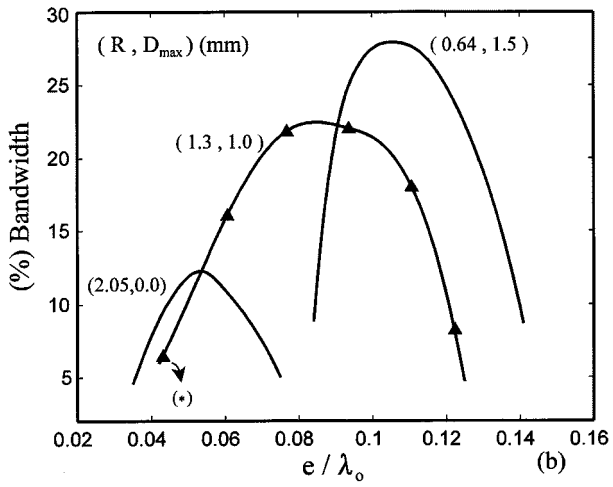

Fig. 4. Active input impedance (a) of the infinite array defined in Fig. 1 for $R = 1.3$ mm, $D_{\max} = 1.0$ mm and different substrate thickness (e/λ_o) given in (b) (▲). The gap substrate thickness e_2 is varied to eliminate the probe inductance in each case. The relative bandwidth for a SWR < 2.0 versus substrate thickness is represented for the previous case and another two different combinations $(R, D_{\max})$.

and to achieve a design procedure in order to enhance the bandwidth impedance of the antenna. First, distinct simulations have been performed for a same total substrate thickness $(e = e_1 + e_2 = 6$ mm) with $\varepsilon_{r1} = \varepsilon_{r2} = 2.55$ and different situations defined in the Table I. The capacitor patch elements are joined to the center conductor of a 50-Ω SMA connector. All the dimensions and dielectric constant of the connector given in Fig. 1 are considered in the computations. The results in Fig. 2 show the active input impedance at broadside in case of direct junction probe-radiating patch (curve a) and with electromagnetic coupling (curves b, c, and d) corresponding to three different combinations $e_1 - e_2 - R$. The curves illustrate the known effect of the series capacitor that produces a counterclockwise rotation on the Smith chart of the input impedance. For the three cases (b, c, and d) the impedance is purely resistive and maximum at the same resonant frequency 5.04 GHz, which has been shift from case a (5.39 GHz). An identical resonant frequency reduction is accomplished. The initial positive reactance of the radiating elements on a thick substrate is compensated and the resistive component appreciably reduced. However, the series capacitor value will be different for each case since it compensates a distinct inductive component proportional to the probe length e_1.

Thus, by adjusting R and e_2, a same reactance compensation from the case of the direct junction may be achieved with different input resistance at resonance with zero reactance. The observation of the curves shows that the resistive component reduction is proportional to the gap substrate thickness and therefore to the capacitor patch radius. As it is well known, the probe location (length s in Fig. 1) may be moved in the appropriate way to compensate this reduction and to match the input impedance. With the same effect, and with a smaller technological complexity, it is proposed a displacement of the radiating patch toward the wall cavity, as shown in Fig. 3, to achieve an optimal matching. The possible effect of the proximity between the patch and the cavity is taken directly into account from the full wave method employed. In this way, the curves e and f in Fig. 2 correspond to the previous cases c and d, but with a patch displacement $D = 1.0$ and 1.5 mm, respectively. Note that the capacitive patch size (R) will limit this displacement if it must remain covered under the radiating patch. There will be a maximum value of D $(D_{\max})$ for given radius R and then the resistive component reduction cannot be compensated indefinitely as the substrate thickness is increased. The Fig. 4(a) shows this fact. The active input impedance is represented for fixed values of $R = 1.3$ mm and $D_{\max} = 1.0$ mm and different substrate thickness given on Fig. 4(b) in the corresponding curve. Each triangle (▲) in this figure corresponds to a curve in Fig. 4(a), being the first one

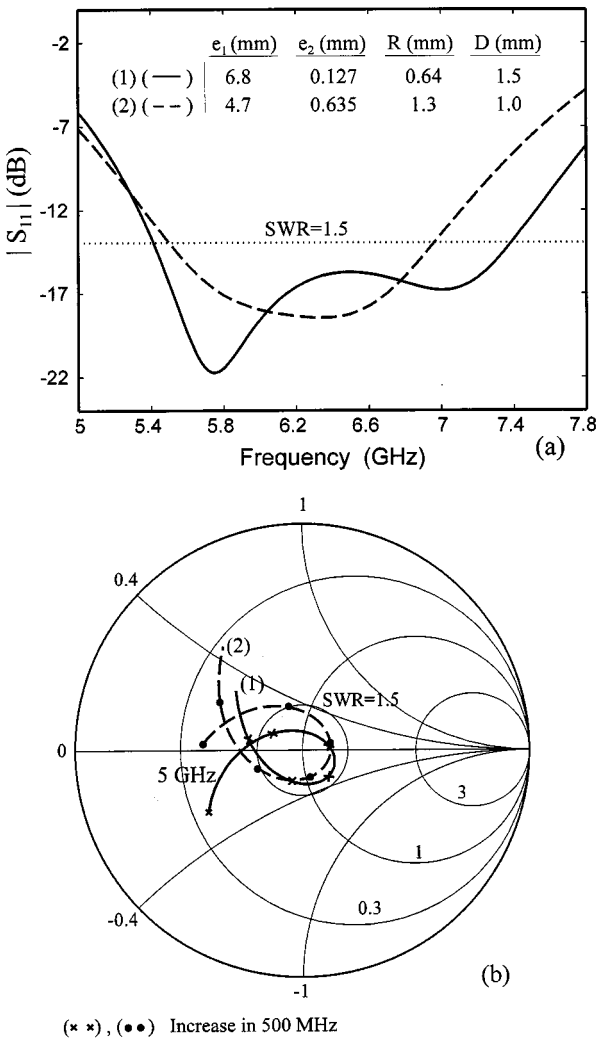

Fig. 5. (a) Broadside active reflection coefficient magnitude and (b) active input impedance of the infinite array shown in Fig. 1 for two different designs defined in Table II.

marked with an asterisk ($*$) on both figures. The capacitive compensation is adjusted in each case by varying e_2 so that the reactive component is canceled at resonant frequency. Thus, for a given size (R) of the capacitor patch there will be an optimum substrate thickness for which a maximum bandwidth is obtained as shown the results in Fig. 4(b). In this figure, the 2.0 standing wave ratio (SWR) bandwidth versus the substrate thickness is depicted for three different cases corresponding to three couples (R, $D_{\max}$). The results illustrate that from a certain substrate thickness, different in each case and smaller as R is increased, a thicker substrate does not produce a bandwidth enhancement owing to the resistive component reduction. Impedance bandwidths larger than those predicted in [1] are attained. Thus, with smaller capacitor patches, it will be possible to match the input impedance with thicker substrates and then to obtain a greater bandwidth. However, the mechanic tolerance of the capacitive patch and gap layer will be more critical. A rectangular patch with an aspect ratio $W/L < 1$ could be chosen to increase the resistance of the patch, which allows to obtain a greater bandwidth with a thicker substrate, although the directivity of the radiating system would decrease owing to the smaller new aspect ratio of the patch.

B. Broad-Band Patch Antenna Designs using Very Low Permittivity Materials

In this section, and based on the previous conclusions, cavity-backed and capacitively probe-fed microstrip antennas on thick substrates are combined with the use of very low permittivity materials to illustrate the substantial bandwidth enhancement that may be obtained without a significant detriment to the radiation properties. Hard foam materials with a low weight and a low permittivity ranging ($\varepsilon_r = 1.03-1.1$) are employed in the design of microstrip antennas to prevent surface wave propagation and to increase the bandwidth [1], [13]. As metal patches cannot be deposited directly on these materials, an additional thin dielectric layer placed on top of the foam may be used to support the radiating elements as shown in [13]. This substrate arrangement may be employed for the structure analyzed in this work: the radiating and capacitor patches will be done on a standard substrate and this one placed over a thick and hard foam substrate. In this way, the permittivity and thickness tolerances of the gap substrate, critical to determine the series capacitance, are fixed by commercial substrates.

Next, results for two distinct designs obtained from two different tetrafluorethylen (PTFE, $\varepsilon_{r_2} = 2.55$) commercial dielectrics employed as gap substrate and a foam substrate with $\varepsilon_{r1} = 1.05$ are presented. The Fig. 5(a) and (b) show the broadside active reflection coefficient magnitude and the active input impedance respectively. The designs have been obtained in each case from a fixed capacitor patch radius and the corresponding maximum patch displacement by choosing between the different commercial PTFE substrate thickness and by adjusting the foam substrate thickness. The adjustment also may be achieved by varying the radius R with commercial thickness of the PTFE and foam substrates. The simulated antenna parameters for each case are given in Table II and Fig. 1.

In the first proposed design the bandwidth for a SWR < 1.5 is 2 GHz, giving a relative bandwidth of 31.3% at the central frequency of 6.4 GHz ($e/\lambda_o = 0.145$). The element spacing corresponds to $0.416\lambda_o$ at this frequency. In the second case, the bandwidth is 1.47 GHz, giving a relative bandwidth of 23.6% at the central frequency 6.23 GHz ($e/\lambda_o = 0.113$). The active element pattern of the electric field is depicted in Fig. 6(a) in E- and H-planes at 6.4 GHz for the first cavity-backed array. A very low H-plane cross-polarization level is obtained and no radiation pattern distortion appears that could be expected owing to the asymmetry of the patch in the cavities. The E-plane cross-polarization level is negligible. Fig. 6(b) shows the broadside-matched active reflection coefficient magnitude Γ versus the scan angle in E- and H-planes at the same frequency. A very good scan performance in the E-plane is observed. The antenna has a scan angle range near 154° for a SWR < 1.5 in this plane. For the same array with a conventional infinite substrate, a substantial reduction in the scan coverage may be expected as shown in [4]. The metal cavities and the low permittivity of

TABLE II
SIMULATED PARAMETERS FOR THE ARRAY SHOWN IN FIG. 1

Design	Foam (ε_{r1}=1.05)	PTFE (ε_{r2}=2.55)	Capacitor patch	Patch displacement
	e_1 (mm)	e_2 (mm)	R (mm)	D (mm)
(1)	6.8	0.127	0.64	1.5
(2)	4.7	0.635	1.3	1.0

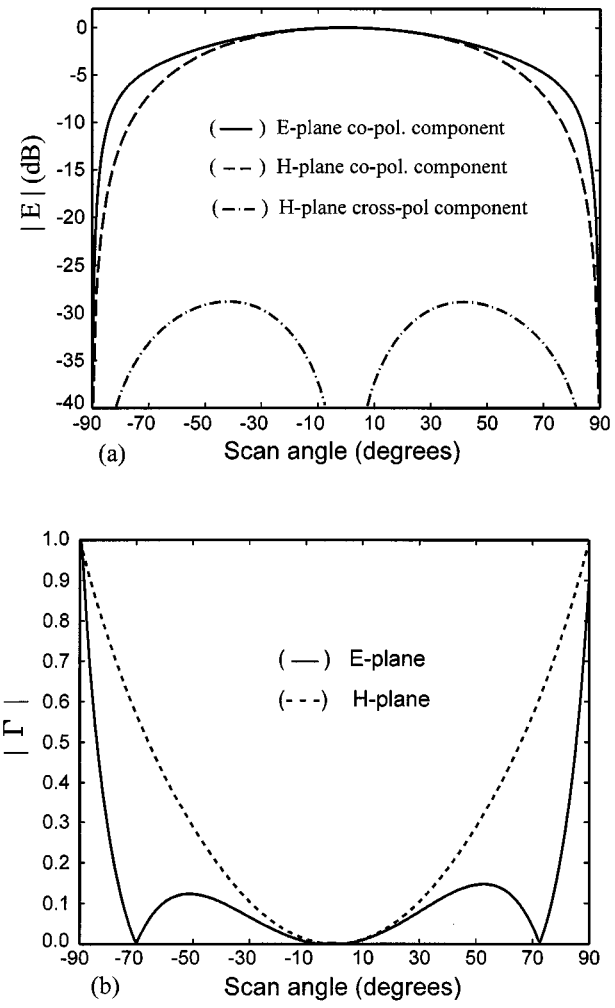

Fig. 6. (a) Normalized active element pattern and (b) broadside-matched active reflection coefficient magnitude versus the scan angle of the infinite array defined in Fig. 1 with the characteristics corresponding to the design (1) in Table II ($f = 6.4$ GHz).

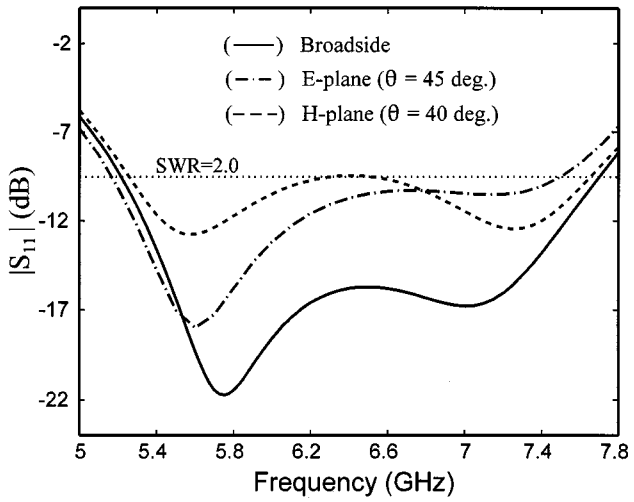

Fig. 7. Active reflection coefficient magnitude versus frequency of the infinite array defined in Fig. 1 (design 1 in Table II) at three different scan angles.

the foam reduce the effect of the surface waves, even with thick substrates, and lead to a scan performance improvement. The active reflection coefficient magnitude versus the frequency is depicted in Fig. 7 for three scan angles (broadside $\theta = 45°$ in E-plane and $\theta = 40°$ in H-plane). A bandwidth of about 35.3% for a SWR < 2.0 is observed over the defined scan volume.

As demonstrated in [10], the bandwidth characteristic of a microstrip antenna array is depreciated as the element spacing is increased. The previous considered array has been analyzed for increasing the periodicity in x direction ($a = 0.5\lambda_o$ and $0.512\lambda_o$ at the frequency of 6.4 GHz) and a relative bandwidth of 24.2 and 22.8% for a SWR < 1.5 have been obtained. The patch displacement has been modified to $D = 1.0$ mm to achieve an optimum bandwidth. In Fig. 8, the active reflection coefficient magnitude and the normalized active element pattern versus the scan angle in the H-plane are depicted for both cases. A considerable scan coverage improvement and an increment of the cross-polarization level are observed in comparison with the previous smaller periodic case. The appearance of a grating lobe at the 72.38° scan angle improves the scan coverage but also produces a radiation pattern distortion. A similar scan performance in the E-plane, depicted in Fig. 6(a) is obtained for the three considered periodicities since the element spacing in y direction has not been modified.

IV. CONCLUSION

A hybrid MM-GSM-FE numerical technique has been employed to analyze capacitive probe fed microstrip patch arrays on thick dielectric substrates and backed by metallic cavities. It is found that this microstrip antenna structure allows to use thicker substrates to enhance the frequency bandwidth without the detrimental effects owing to the surface wave excitation. The effect of the capacitive coupling has been investigated and different broad-band designs have been presented. It is found that with smaller capacitor patches it is possible to achieve greater

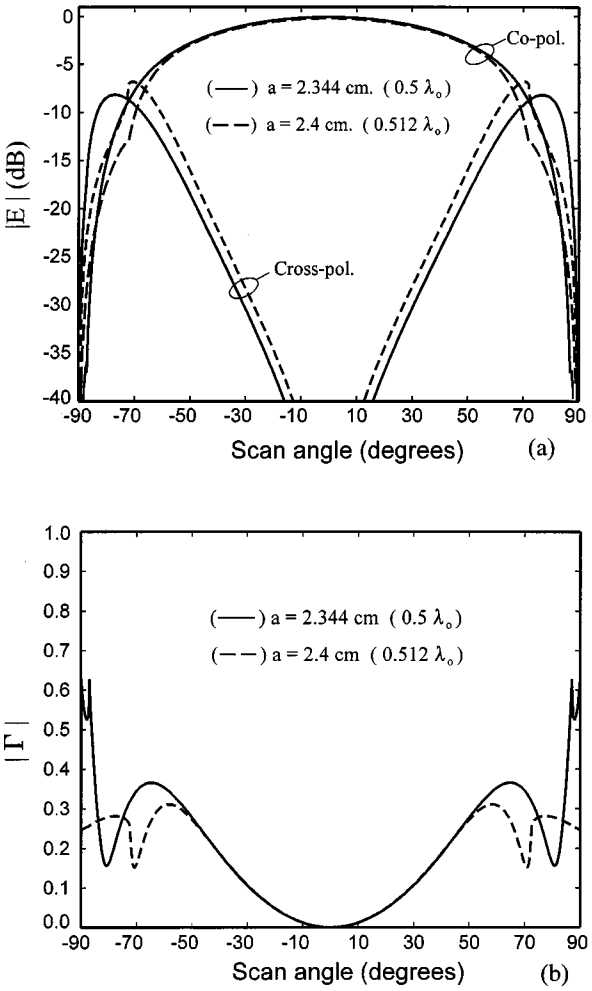

Fig. 8. (a) Normalized active element pattern and (b) broadside-matched active reflection coefficient magnitude versus the scan angle in the H-plane, of the infinite array defined in Table II (design 1) with two different element spacing "a" in x direction ($f = 6.4$ GHz).

bandwidths. The reduction of the element spacing that leads to a bandwidth enhancement, also produces a decrease of the cross-polarization level and a diminution of the scan coverage.

REFERENCES

[1] D. M. Pozar, "A review of bandwidth enhancement techniques for microstrip antennas," in *Microstrip Antennas*. Piscataway, NJ: IEEE Press, 1995, ch. 4.

[2] D. M. Pozar and D. H. Schaubert, "Analysis of an infinite array of rectangular microstrip patches with idealized probe feeds," *IEEE Trans. Antennas Propagat.*, vol. AP-32, pp. 1101–1107, Oct. 1984.

[3] E. Chang, S. A. Long, and W. F. Richards, "An experimental investigation of electrically thick rectangular microstrip antennas," *IEEE Trans. Antennas Propagat.*, vol. AP-34, pp. 767–772, June 1986.

[4] F. Zavosh and J. T. Aberle, "Infinite phased arrays of cavity-backed patches," *IEEE Trans. Antennas Propagat.*, vol. 42, pp. 390–398, Mar. 1994.

[5] M. Davidovitz, "Extension of E-plane scanning range in large microstrip arrays by substrate modification," *IEEE Microwave Guided Wave Lett.*, vol. 2, pp. 492–494, Dec. 1992.

[6] J. M. Jing and L. Volakis, "A hybrid finite element method for scattering and radiation by microstrip patch antennas and arrays residing in a cavity," *IEEE Trans. Antennas Propagat.*, vol. 39, pp. 1598–1604, Nov. 1991.

[7] J.-C. Cheng, N. I. Dib, and L. P. B. Katehi, "Theoretical modeling of cavity-backed patch antennas using a hybrid technique," *IEEE Trans. Antennas Propagat.*, vol. 43, pp. 1003–1013, Sept. 1995.

[8] K. S. Fong, H. F. Pues, and M. J. Withers, "Wideband multilayer coaxial-fed microstrip antenna element," *Electron. Lett.*, no. 21, pp. 497–499, 1985.

[9] P. S. Hall, "Probe compensation in thick microstrip patches," *Electron. Lett.*, no. 23, pp. 606–607, 1987.

[10] A. K. Bhattacharyya, "A modular approach for probe-fed and capacitively coupled multilayered patch arrays," *IEEE Trans. Antennas Propagat.*, vol. 45, pp. 193–202, Feb. 1997.

[11] M. González, J. A. Encinar, J. Zapata, and M. Lambea, "Full wave analysis of cavity-backed and probe-fed microstrip patch arrays by a hybrid mode-matching, generalized scattering matrix and finite-element method," *IEEE Trans. Antennas Propagat.*, vol. 46, pp. 234–242, Feb. 1998.

[12] M. A. González, J. A. Encinar, and J. Zapata, "Radiation pattern computation of cavity-backed and probe-fed stacked microstrip patch arrays," *IEEE Trans. Antennas Propagat.*, vol. 48, pp. 502–509, Apr. 2000.

[13] J. F. Zürcher, "The SSFIP: A global concept for high-performance broadband planar antennas," *Electron. Lett.*, vol. 2, no. 23, pp. 1433–1435, Nov. 1988.

Miguel A. González de Aza was born in Madrid, Spain. He received the Ingeniero de Telecomunicación and Ph.D. degrees, both from the Universidad Politécnica de Madrid, Spain, in 1989 and 1997, respectively.

From 1990 to 1992, he has been with the Departamento de Electromagnetismo y Teoría de Circuitos, Universidad Politécnica de Madrid, with a research scholarship from the Spanish Ministry of Education and Science. He became an Assistant Professor in 1992 and Associate Professor in 1997, at the same university. His main research interests include analytical and numerical techniques for the analysis and characterization of waveguide structures and microstrip antennas.

Juan Zapata (M'93) received the Ingeniero de Telecomunicación and the Ph.D. degrees, both from the Universidad Politécnica de Madrid, Spain, in 1970 and 1974, respectively.

Since 1970 he has been with the Departamento de Electromagnetismo y Teoría de Circuitos, Universidad Politécnica de Madrid, where he became an Assistant Professor in 1970, Associate Professor in 1975, and Professor in 1983. He has been engaged in research on microwave active circuits and interactions of electromagnetic fields with biological tissues. His current research interest include computer-aided design for microwave passive circuits and numerical methods in electromagnetism.

José A. Encinar (S'81–M'86) was born in Madrid, Spain. He received the Electrical Engineer and Ph.D. degrees, both from Universidad Politécnica de Madrid (UPM), Spain, in 1979 and 1985, respectively.

Since January 1980 has been with the Applied Electromagnetism and Microwaves Group at UPM, as a Teaching and Research Assistant from 1980 to 1982, as an Assistant Professor from 1983 to 1986, and as Associate Professor from 1986 to 1991. From February to October of 1987 he was with the Polytechnic University, Brooklyn, NY, as a Postdoctoral Fellow of the NATO Science Program. Since 1991 he has been a Professor in the Electromagnetism and Circuit Theory Department, UPM. In 1996 he was with the Laboratory of Electromagnetics and Acoustics at Ecole Polytechnique Fédérale de Lausanne (EPFL), Switzerland, as Visiting Professor. His research interests include analytical and numerical techniques for the analysis and design of waveguide structures, frequency selective surfaces, and multilayer printed arrays.